

PAPER • OPEN ACCESS

Magnification of energy transmission ratio using miniature cycloidal gear box for humanoids

To cite this article: Umesh Chavan *et al* 2022 *IOP Conf. Ser.: Mater. Sci. Eng.* **1272** 012017

View the [article online](#) for updates and enhancements.

You may also like

- [A manufacturing error measurement methodology for a rotary vector reducer cycloidal gear based on a gear measuring center](#)
Tianxing Li, Junxiang Zhou, Xiaozhong Deng et al.
- [The origin of the large magnetoelectric coupling in the ceramic \$\text{Ba}_0.7\text{Bi}_0.3\(\text{Ti}_0.5\text{Zr}_0.5\)\text{Fe}_0.9\text{O}_3\$](#)
Imen Kallel, Hamadi Khemakhem, Zina Sassi et al.
- [Structure and spin dynamics of multiferroic \$\text{BiFeO}_3\$](#)
Je-Geun Park, Manh Duc Le, Jaehong Jeong et al.



Connect with decision-makers at ECS

Accelerate sales with ECS exhibits, sponsorships, and advertising!

▶ Learn more and engage at the 244th ECS Meeting!

Magnification of energy transmission ratio using miniature cycloidal gear box for humanoids

Umesh Chavan¹, Atharv Joshi², Yash Kolambe², Harsh Gwalani², Harish Chaudhari², Aniket Khalate², Pravin Hujare³

^{1,2} Department of Mechanical Engineering, Vishwakarma Institute of Technology
Pune, Maharashtra, India

³ Department of Mechanical Engineering, Vishwakarma Institute of Information
Technology,
Pune, Maharashtra, India

Abstract. Design challenges arise in applications like humanoids where high torque is required to move and self-balance the bot. Present research focuses on development of a cycloidal gearbox for humanoid shoulder joints. Light weight gear box assembly was designed with mass of 360g. Structural design and analysis of cycloidal gearbox is carried out. A 3D printed prototype is developed to validate motion analysis. It was actuated by NEMA 17 step motor (0.45 N-m) which is controlled by A4988 motor driver module on the Arduino platform. The speed reduction ratio is achieved 20:1 in a very small space of 60 x 60 x 20mm. Motor torque 0.45Nm is magnified up to 8.82Nm. Result shows proposed cycloidal gearbox satisfies requirement of humanoid shoulder joints such as high torque, light weight and compact assembly. Additional features noticed are back drivable, vibration and noise free transmission which are highly desirable for humanoid shoulder joints.

Keywords: Torque, Cycloidal Gearbox, Humanoid, Motion study, 3D printing

1. Introduction

Robotics is a multi-disciplinary domain where mechanical, electronics, and computer science work together to get the best possible solution. In robotic arms, high torque is required at the output for holding larger loads. To increase the torque of the motor, it is essential to use a gearbox which can efficiently increase the torque in a very small amount of space. There are various gearboxes available which are very compact and can also transmit power at a very high reduction ratio (in the range of 100 and above). For instance, García et al. [1] proposed a review on the performance of harmonic and cycloid drives, along with emerging transmission technologies such as REFLEX torque amplifier, Archimedes drive, Nugear, Bilateral drive, Galaxie drive etc. used in modern robotics. Jonathon W. Sensinger and James H. Lipsey [2] also compared cycloidal and harmonic drives. Study done by Biser Borislavov et al. [3] Study shows designing of a cycloidal reducer. Mirko Blagojevic et al. [4] presented a new concept of the two-stage cycloidal speed reducer development. Logan C. Farrell et al. [5] vibrations caused due to gearbox results in noise and affects its overall life. If a single plate is used, a counter balance must be added to avoid substantial vibration. Mathematical model and design procedures to design the epicycloid planet gear of cycloid drives was discussed by Ta-Shi Lai [6]. Wei Bo et al. [7] carried out load distribution model and presented equation for design. Following researchers presented some of the potential applications of cycloidal geometry based power transmission benefits and issues. Abhi J.



Rawal [8] developed cycloidal based drive joint for wearable exoskeletons. Hiroshi Matsuki et al. [9] presented bilateral drive gear that is highly back drivable reduction gearbox for robotic actuators. Benedetto Allotta et al. [10] redesigned the cycloidal drive for novel applications in machines. Li, X. et al. [11] and Wan-Sung Lin et al. [12], presented design of a two-stage cycloidal gear reducer with tooth modifications. Li Yawei and Wu Yuanzhe [13] developed RV reducer i.e. one type of cycloid reducer. [14] In this paper, methodology was developed to draw cycloidal gear in minutes and also reduces the possibility of human error and the time to draw each gear which is the main fact why the wider use of cycloidal gears is limited. Stress analysis of cycloidal speed reducer was done by using Finite Element Method (FEM) for the case of single meshing which is the most critical case. Experimental analysis was carried using the strain gauges method [15]. Kinematic analysis of cycloidal speed reducer was performed using the softwares – Autodesk Inventor and Solidworks [16]. In the research work [17] modelled in a dynamic simulation environment, on the rotating parts of cycloidal reducer. The study [18] gave an insight about the internal load sharing of the rotating parts and their capability of carrying the shock loads of cycloidal gears. Present work focuses on the design of a cycloid power transmission unit (gearbox) that possess characteristics of a high reduction ratio in a very compact assembly, much less weight and operating reliably with very less vibrations for humanoid shoulder joints. Computer codes are developed to get the cycloidal profile. A 3D printed prototype is produced to perform tests and validate motion analysis. In order to reduce the vibrations, two cycloidal discs are used which have a phase difference of 180° . It was actuated by NEMA 17 step motor (0.45 N-m) which is controlled by A4988 motor driver module on the Arduino platform.

2. Creative Design of Cycloidal Gearbox

2.1 Conceptual design

Conceptual design of cycloidal gearbox (CG) shown in Fig. 1. It consists of an eccentric camshaft (input shaft), cycloidal gears, annular cycloidal gear (output gear), flange, fasteners (pins) and motor. Exploded view shown in Fig. 1 elaborates power transmission elements involved in CG. Fig. 2 shows assembly of proposed gearbox with motor drive. An eccentric camshaft transmits motor power to annular gear through cycloidal gears. Which drives a cycloidal gears. In present work as a case study, torque requirement of humanoid shoulder joint is considered to design CG. Requirement is to magnify the motor torque by 20 times. This implies when eccentric cam shaft rotates in 360° annular cycloidal gear must rotate 18° , so that after 20 rotations of the input shaft, the output shaft completes one rotation. Thus cycloidal gear box is designed for the transmission ratio of 20:1

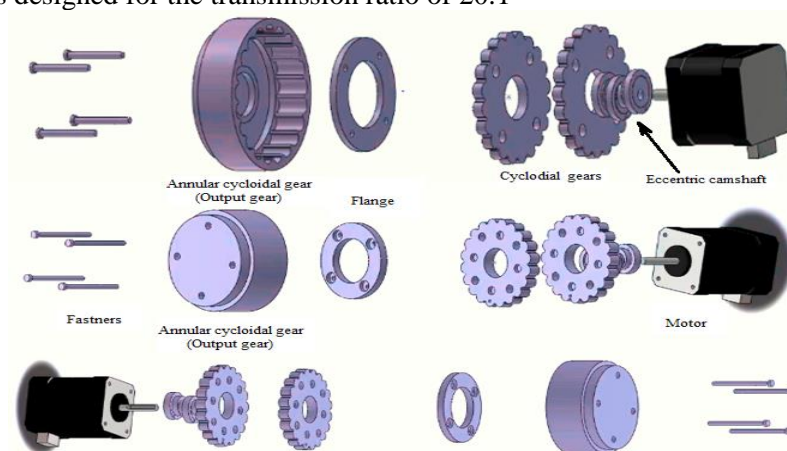


Figure 1. Major elements of proposed cycloidal gearbox (CG)

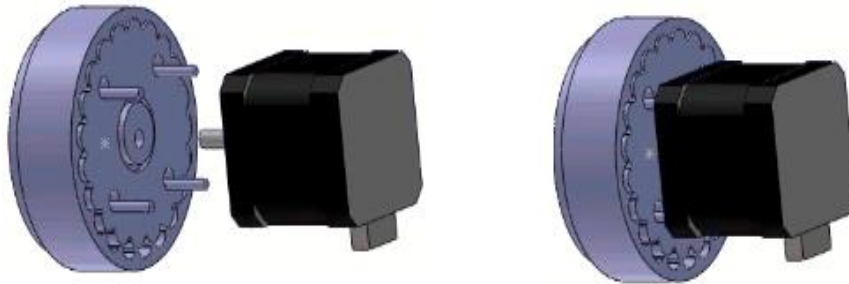


Figure 2. Assembled view of proposed cycloidal gearbox (CG)

2.2 Generation of cycloidal profile

The rotor has a very unique cycloidal shape. There are standard equations available to design the profile of the rotor [13]. The parametric curve equations were chosen because of the two equations needed to define the rotor as shown in Fig. 3. Once the rotor radius (R), eccentricity (E), roller radius (R_r), and the number of rollers (N) is set, the given equations can then be used to generate cycloidal rotor profile coordinates C_x and C_y (X and Y respectively)

$$X = R \cos(\theta) - R_r \cos(\theta - \psi) - E \cos(N\theta) \quad (1)$$

$$Y = -R \sin(\theta) + R_r \sin(\theta - \psi) + E \sin(N\theta) \quad (2)$$

$$\psi = -\tan^{-1} \left[\frac{\sin((1-N)\theta)}{\left(\frac{R}{EN}\right) - \cos((1-N)\theta)} \right] \quad (3)$$

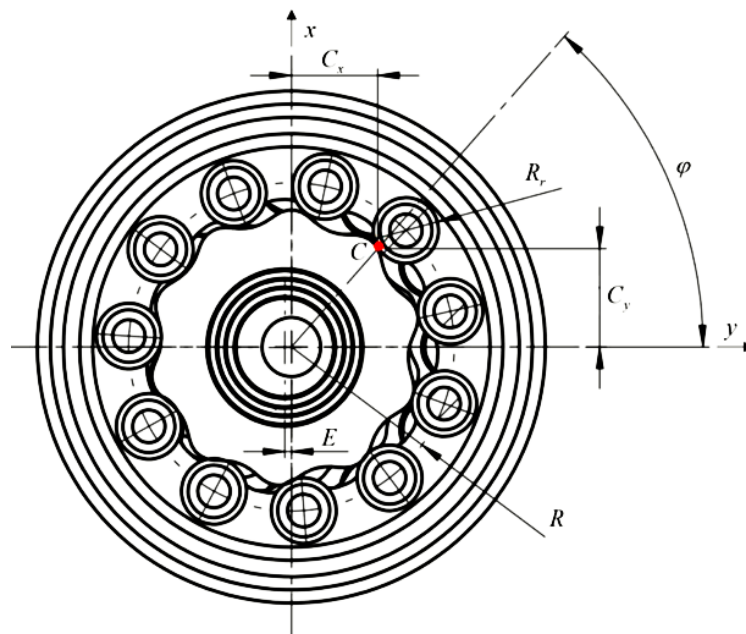


Figure 3. Cycloidal gear profile generation parameters

Contact angle between the cycloidal rotor teeth and the rollers ψ . Equation can be utilized to compute the contact angle using different θ values ranging from 0 to 360° . The precision of the rotor profile depends on the step value of the angle θ . In other words, the meshing between rotor teeth and rollers will be precise, resulting in negligible backlash.

Table 1. Cycloidal profile parameters

Parameters	Values
No. of teeth on gear (N)	20
No. of roller pins (n)	21
Rotor radius (R)	30 mm
Roller pin radius(Rr)	3 mm
Eccentricity (E)	1.5 mm

MATLAB code was written to generate the cycloidal profile of gear tooth as shown in Fig. 4. Profile of cycloidal gear is a critical parameter to its design, so developed a software program in MATLAB. It takes the number of lobes and pins as input and uses a constraint that the number of pins are equal to number of lobes plus one. Rotor radius as per packaging was 30mm, eccentricity was again a critical design parameter which was 1.5mm. Using the appropriate equations other parameters were calculated housing circle diameter and transmission ratio. The shape of the rotor is very unique and standard equations are available to design the profile of the rotor. Mainly, two different types of equations are available and can be used, explicit equations and parametric equations. So, the parametric equations have been used here in the code and the angle is varied from -180 degrees to 0 degrees for the lower half and from 0 to 180 degrees for the upper half. This was done to maintain continuity and obtain a smooth profile. The results were also plotted to get a cycloidal profile as can be seen in Figure 4. The main aim behind writing the code was to see the effect that various parameters have on the profile of the rotor, the size of the rotor, the eccentricity, the transmission ratio, etc. without making CAD models for each iteration.

Code:

```
% For Transmission Ratio
n = 20; %Number of Lobes
N = 21; %Number of Pins (Rollers)
% N = n + 1 is the condition

TR = (n/(N - n)); %Transmission Ratio

R = 30; %Rotor Radius

% Housing Circle Circumference
HCC = 2 * R * pi ();

Rr = (HCC/ (4 * N)); %Roller Radius

E = 1.5; %Shaft Eccentricity

for t = linspace (-180, 0, 362)
    X = (R*cosd(t))-(Rr*cosd(t+deg2rad(atan(sind((1-N)*t)/((R/(E*N))-cosd((1-N)*t))))))-(E*cosd(N*t));
    % plot(X, Y, 'r*');
    % hold on;
    Y = (-R*sind(t))+(Rr*sind(t+deg2rad(atan(sind((1-N)*t)/((R/(E*N))-cosd((1-N)*t))))))+(E*sind(N*t));
    plot(X, Y, 'r. ');
    hold on;
end

for t = linspace (0, 180, 362)
    X = (R*cosd(t))-(Rr*cosd(t+deg2rad(atan(sind((1-N)*t)/((R/(E*N))-cosd((1-N)*t))))))-(E*cosd(N*t));
    % plot(X, Y, 'b*');
```

```

% hold on;
Y = (-R*sind(t))+(Rr*sind(t+deg2rad(atan(sind((1-N)*t)/((R/(E*N))-cosd((1-N)*t)))))+(E*sind(N*t));
plot(X, Y, 'g. ');
hold on;
end

```

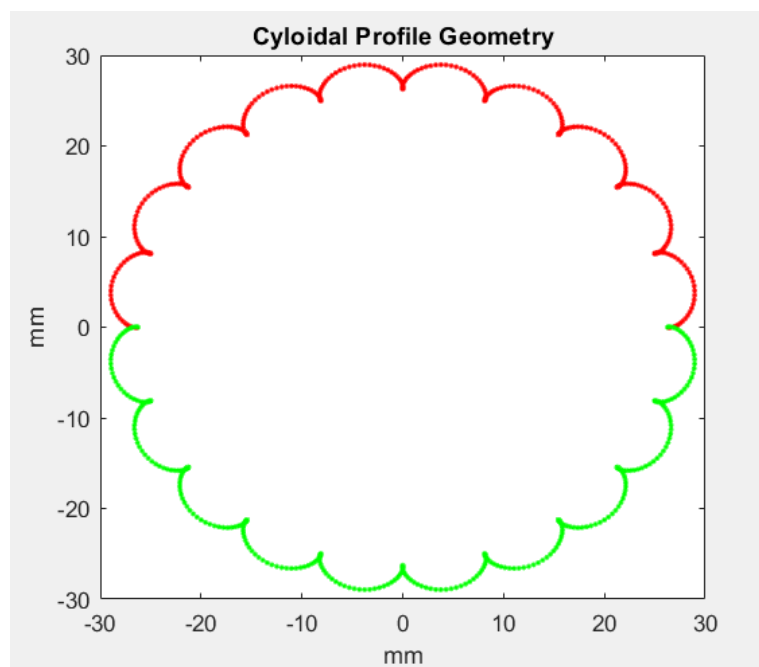


Figure 4. Cycloidal profile generated using code

2.3 Structural Analysis of Cycloidal Gears

Strength analysis of cycloidal rotor (disc) and casing is carried out. Working loads are applied on each of the parts to obtain maximum stress and deformations. Conditions: Fixed – backside of casing (where arm will be seated), force applied - 260 N, Mesh – tetrahedral

Material chosen - Polylactic acid (PLA)

Material properties of PLA

Density : 1.25 g/cm³

Young's modulus : 3027 MPa

Poissions ratio : 0.32

From the analysis as seen in Fig.5, the maximum deformation is of 0.379 mm at the teeth of the output where the cycloidal gear and output completely meshes. The minimum deformation is zero where there is no contact between the cycloidal gear and the output. From the contour plot in Fig.6 , it can be seen that the maximum stress at completely meshed teeth because the force acting at that point is maximum and minimum stress where the gear is not in contact with the output. The minimum stress value is 298Pa and maximum value is 61.82 Mpa. Same is the case for the deformation of the cycloidal gear as it is for the out as observed in the Fig.7. The deformation is maximum at the teeth which is completely meshed with the output and the deformation goes on decreasing equally on both sides of the meshed teeth. The maximum deformation in this case is 0.355mm and minimum of 0mm about the centre of the gear. From the contour plot in Fig. 8 it can be observed that the maximum stress occurs at the root of one teeth that gets completely meshed which is 45.9Mpa. Also the stress occurs between the eccentric shaft and the cycloidal gear which is around 15 MPa.

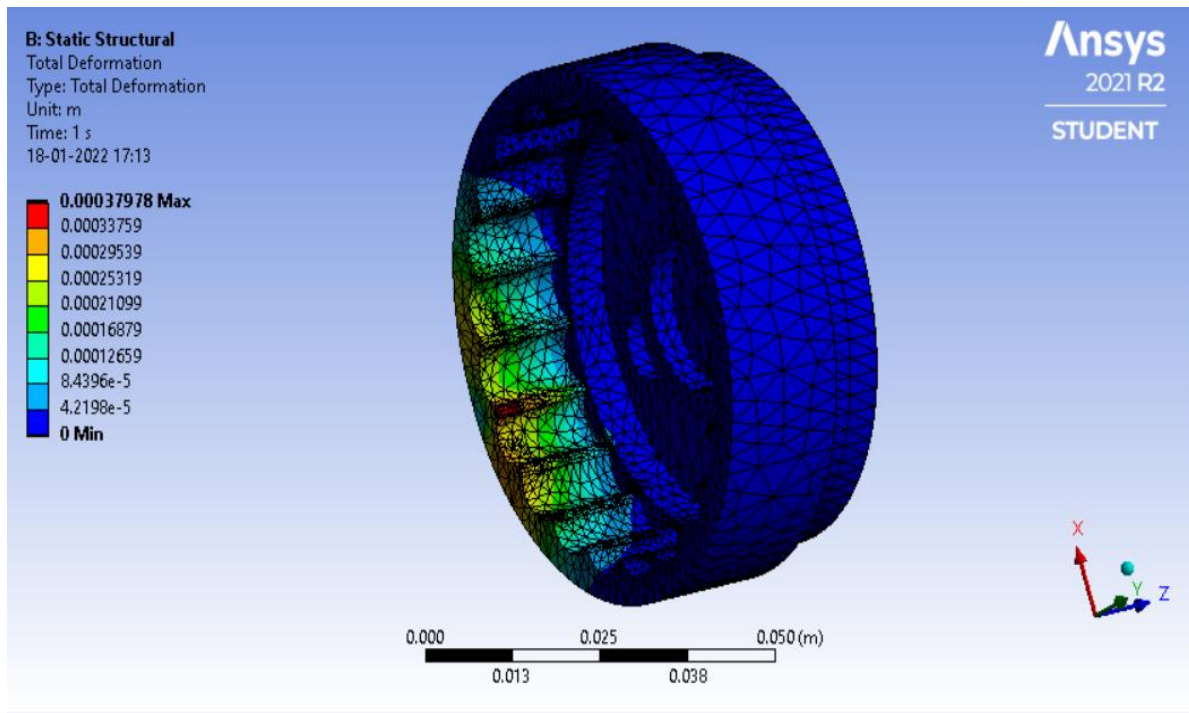


Figure 5. Deformation of annular gear of cycloidal gear box

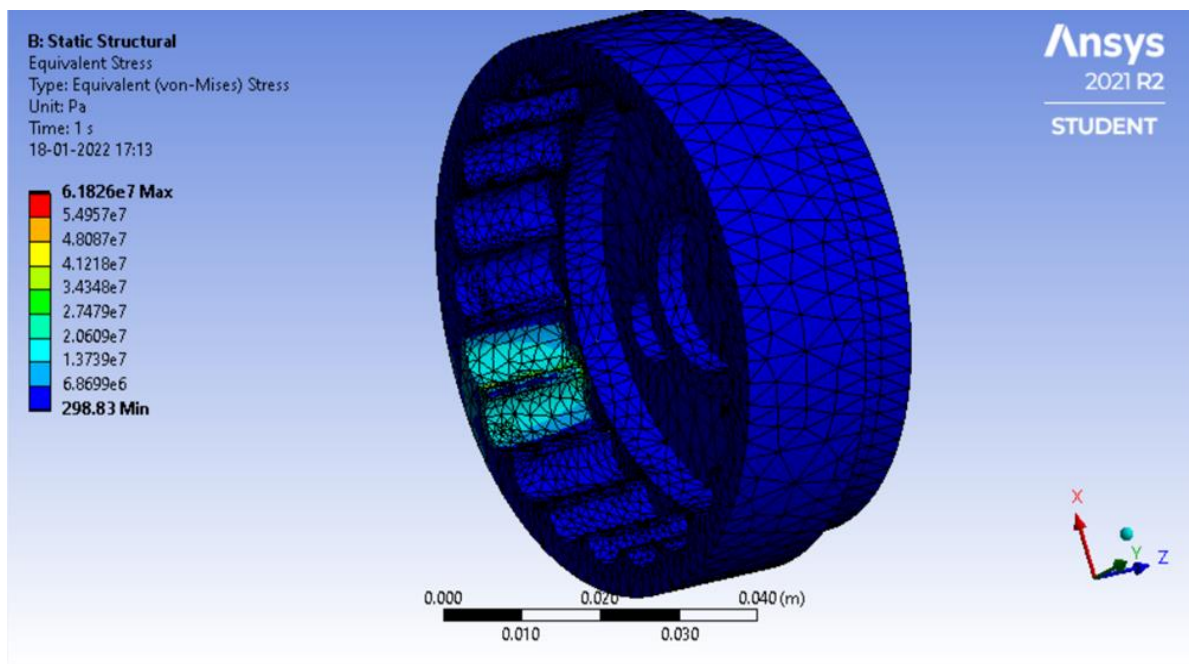


Figure 6. Von-Mises stress on annular gear of cycloidal gear box

Analysis was carried out in Ansys Student Version with following boundary conditions Fixed - Inner bearing face, Force applied - 260 N, Mesh – tetrahedral

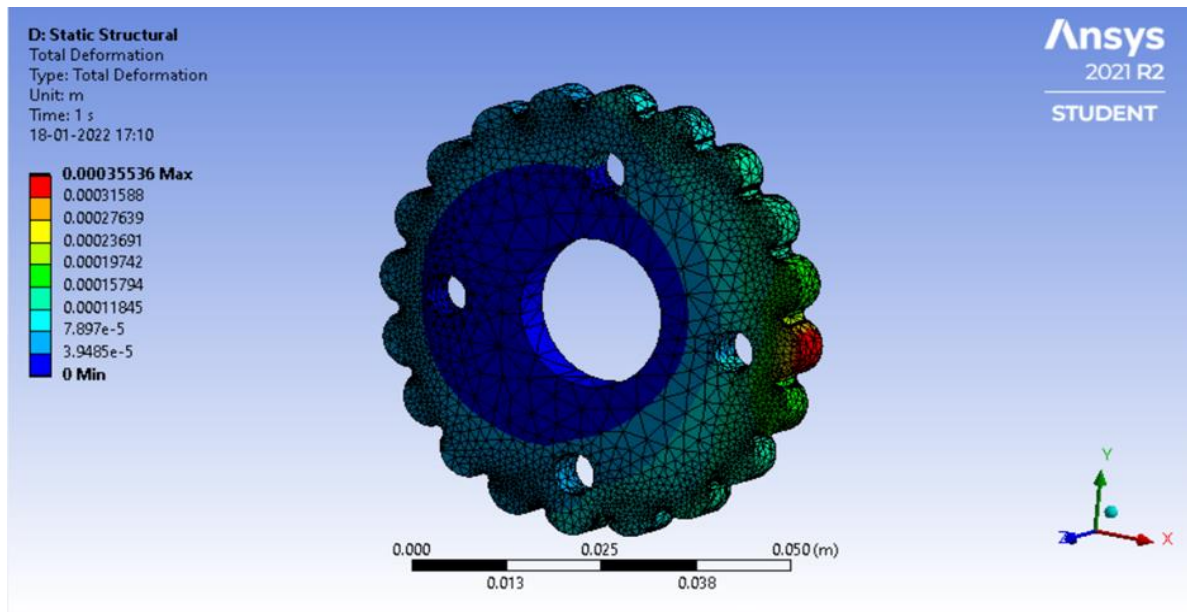


Figure 7. Deformation of cycloidal gear of cycloidal gear box

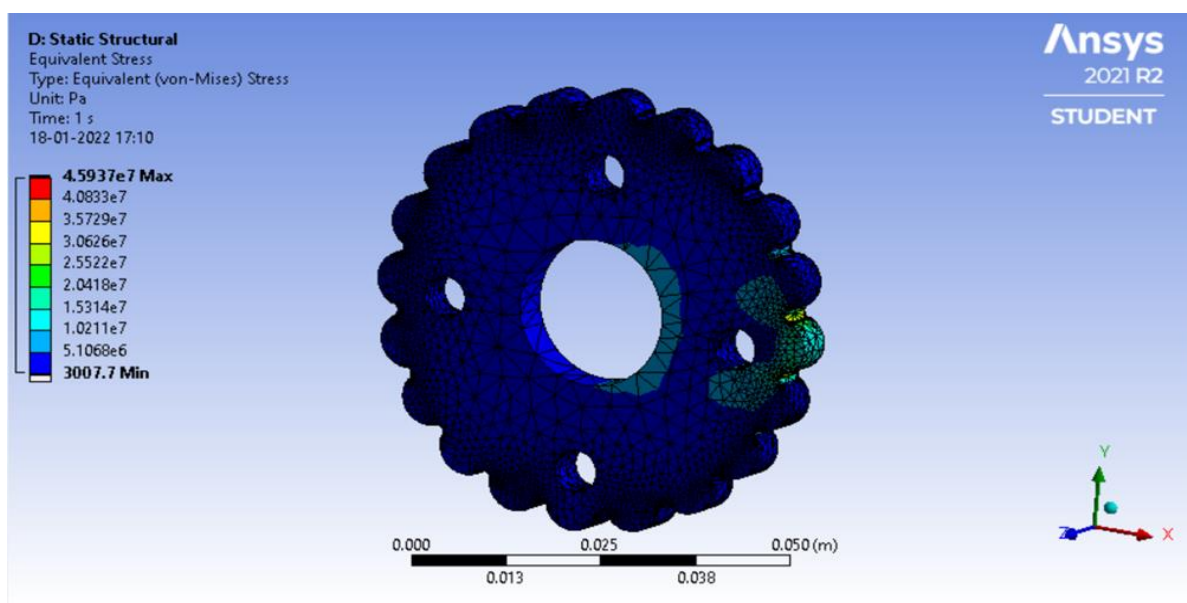


Figure 8. Von-Mises stress on cycloidal gear of cycloidal gear box

The stress levels and deformations found to be within the allowable limits as two out of phase cycloidal gears helps to reduce load distribution on individual gears. Also, contact stress and deformation of the proposed cycloid drive is much hence, proposed cycloid drive exhibits high load capability which is more suitable for robotic arm applications. Thus the structural strength was verified before the developments of prototype.

3. Motion Analysis

Motion study of CG was performed in computational tools. Fixed support boundary condition was given to the bolts and rotary input motion to the eccentric camshaft. Solid body contact assumed between the bearing and the discs, the eccentric shaft and the bearing, the cycloidal gear and the annular gear casing. Gravity condition also applied and a weight attached at the output side. The angular velocity of the output gear found to be one by twenty times of the input angular velocity. Similarly, the output torque

which was derived by using the angular acceleration was also close to the desired values. The humanoid for which this gearbox is designed is going to an interactive entertainment bot with capability of holding 4.5 kg load at 0.2m distance which is equivalent to 7.8Nm. Fig. 9 shows the torque drawn by the motor over time. The values are fluctuating as gravity effect is considered and a single mass (for load) is given at output. Fig. 10 shows the angular velocity obtained at the output shaft. Input speed given to motor was 60 rpm, and the output speed computed was 3.13 rpm (0.3314 rad/s or 19 deg./s). The angular acceleration graph was also plotted shown in Fig. 11. The angular acceleration values obtained for each time step from motion analysis was exported to torque analysis. Here, these values were multiplied the inertia of the output part to calculate the torque that is required by the output (and the load) to rotate at each time step. The graph of torque required at each time step is shown below in Fig. 12.

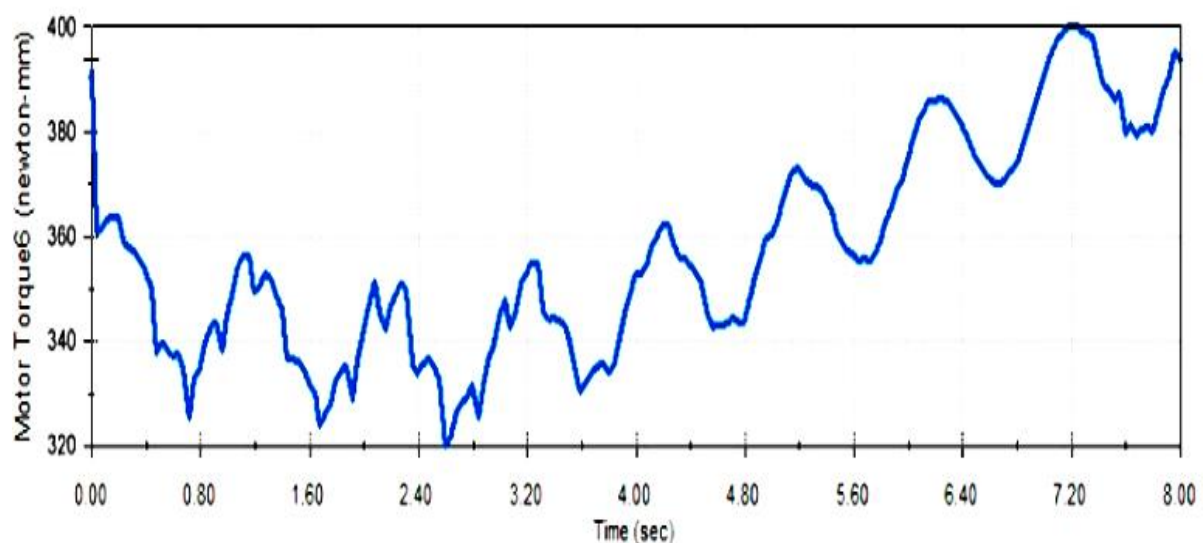


Figure 9. Motor torque vs time (sec.)

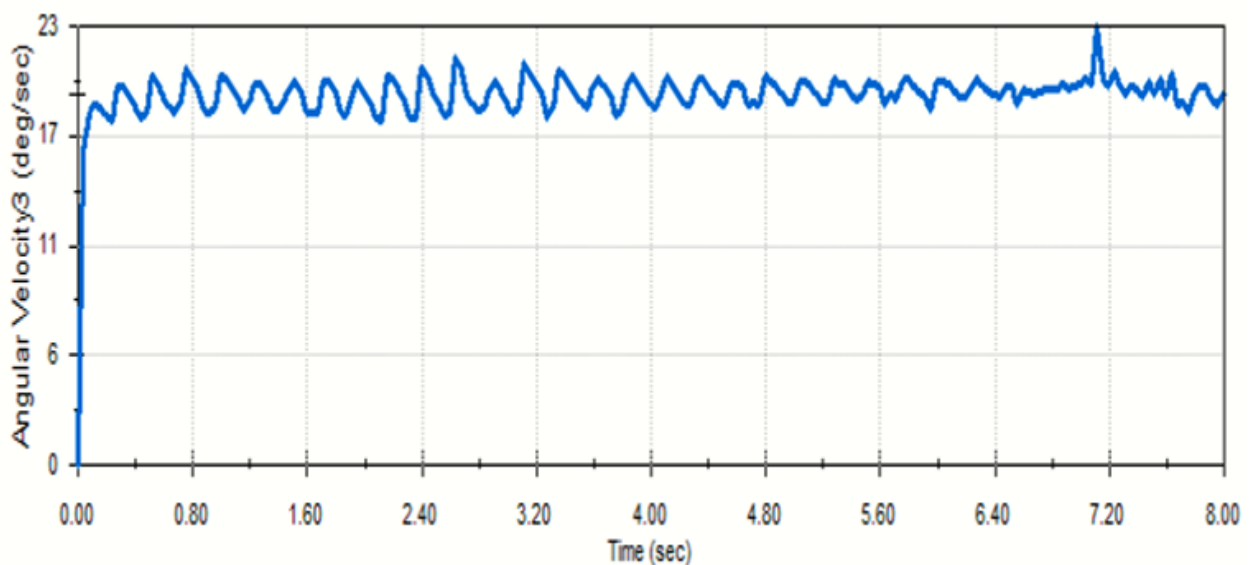


Figure 10. Angular velocity vs time (sec.)

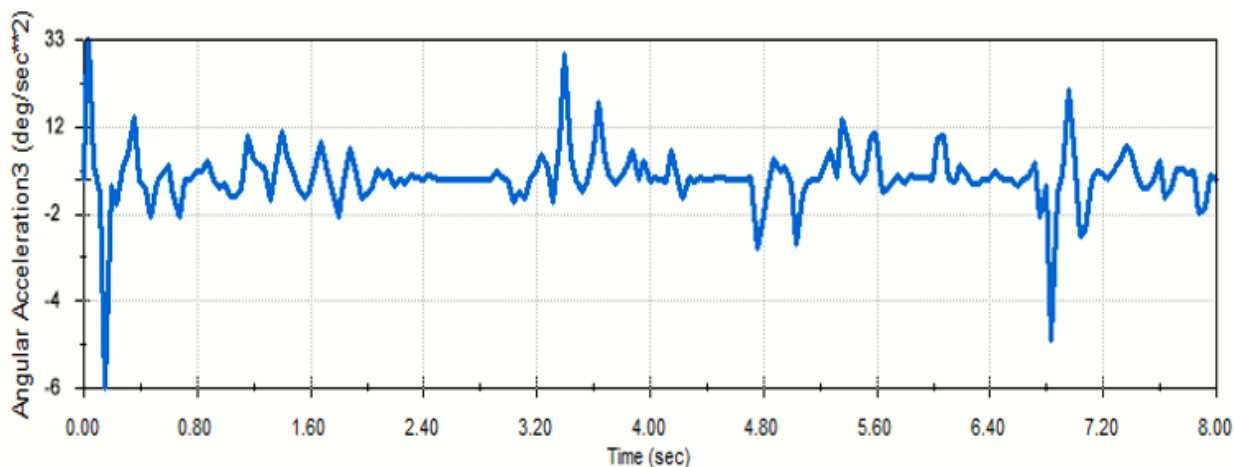


Figure 11. Angular acceleration vs time (sec.)

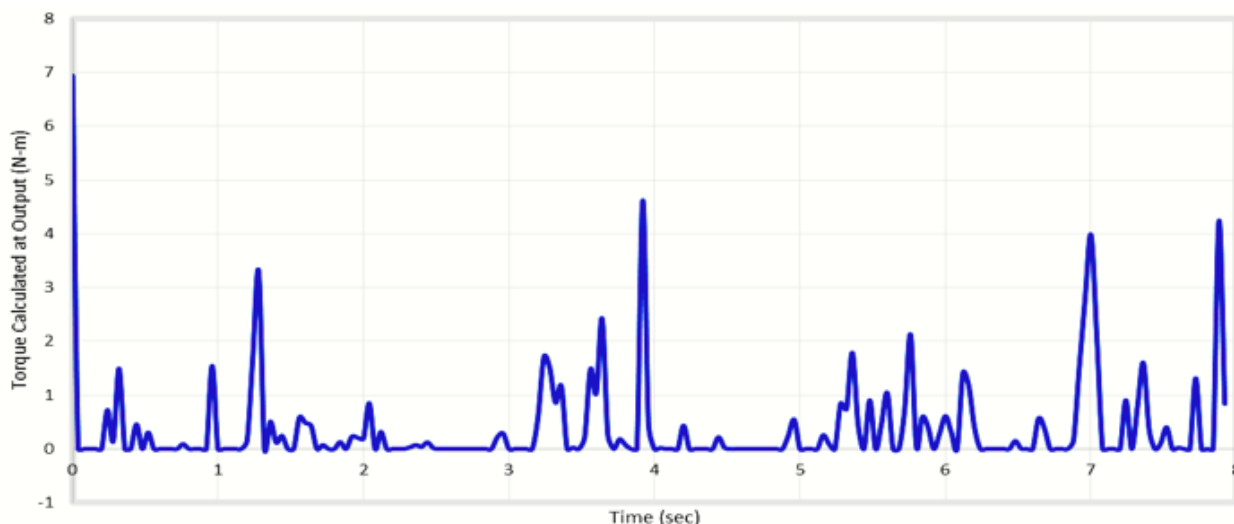


Figure 12. Torque output vs time (Sec)

4. Prototype and Experiments

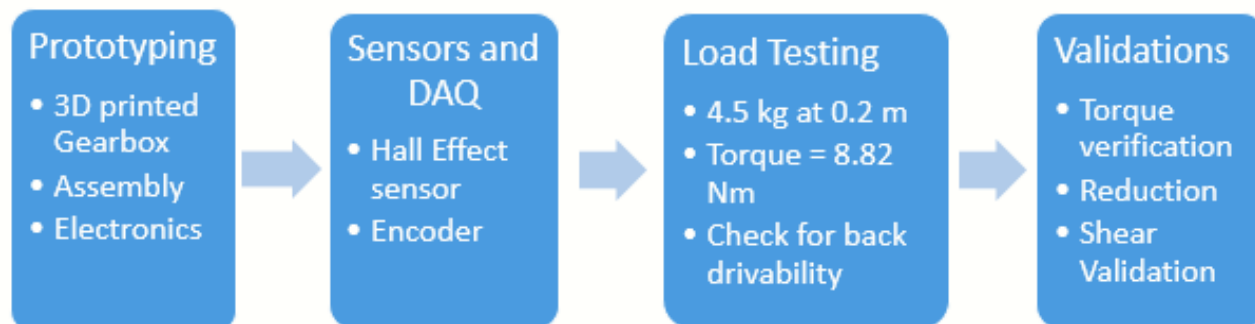


Figure 13. Design of experiment

4.1 Prototyping

Fig. 13 shows design of experiment plan to build and test the CG. As per design specifications a prototype of CG was 3D printed. The parts included the eccentric camshaft, cycloidal gears, annular gears, and casing. 3D printed components shown in Fig. 14. Special care to be taken to make accurate

assembly of all components. Bearings are press fitted in the 3D printed cycloidal discs. Bolts were used as the connectors between the discs and the retainer which will allow the disc to wobble around it. Finally, the cycloidal discs are fitted into the cycloidal casing. Both the discs were mounted on the eccentric shaft in the phase difference of 180° . Input and output covers were also fitted and finally bolted to prepare the final gearbox assembly. Overall space dimensions of a cycloidal gear box was 60 x 60 x 20mm and mass assembly is 360g.

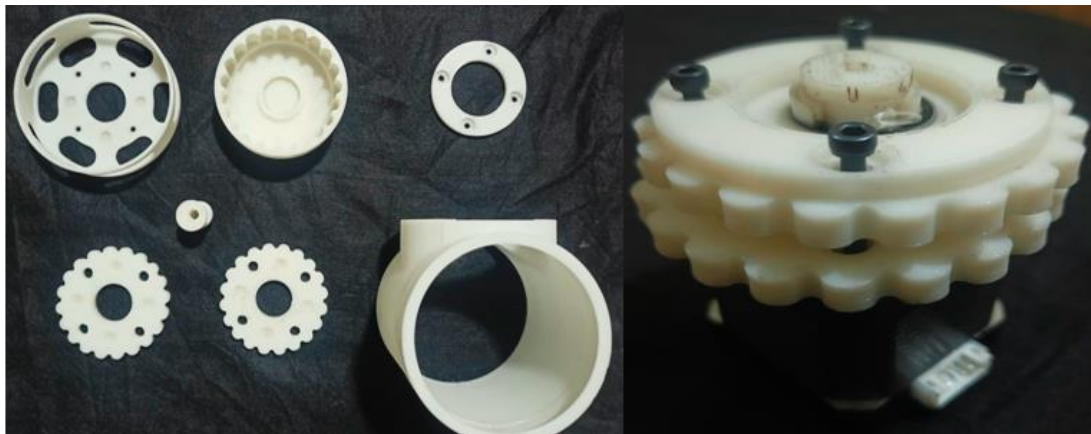


Figure 14. 3D printed components of cycloidal gear box

4.2 Testing setup

Input is given to gearbox using a 12 Volt, 0.45 N-m, NEMA 17 stepper motor. These motors come with an outer casing, which are easy to mount and ensure stable operation. This motor required a special motor driver due to its high ampere rating. A4988 motor controller was used along with the RUDRA board to drive this motor. This motor also allows to vary the speed. This could be done by changing the delay between the consecutive frequency pulses in the code. RUDRA board (which is very similar to the Arduino UNO Micro-controller). External power supply was given to the micro-controller using a 12 V, 2A adaptor.

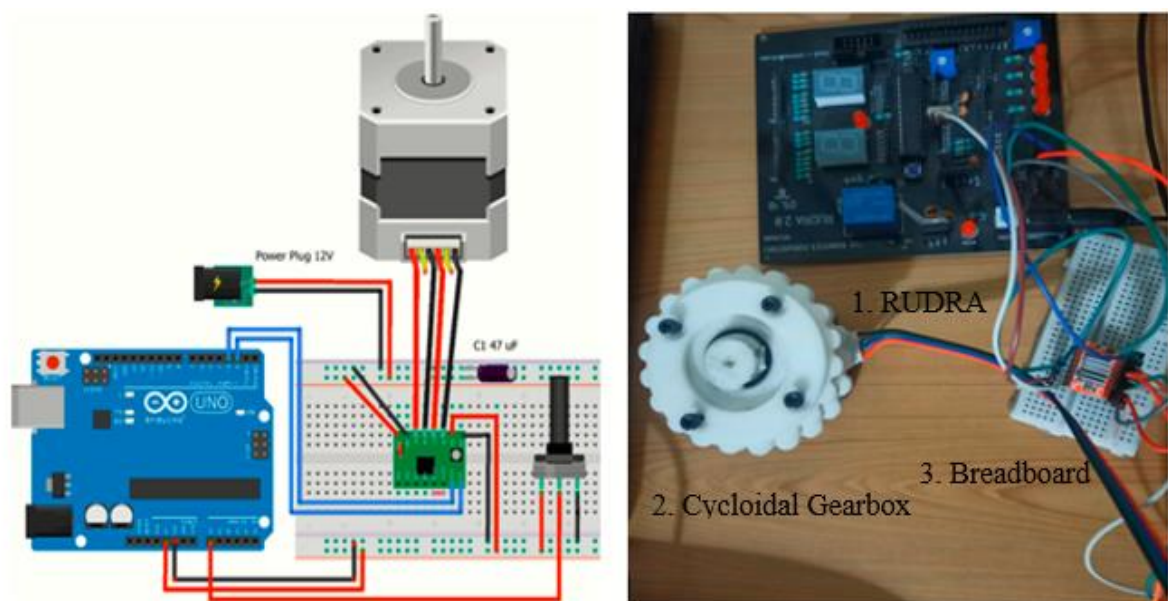


Figure 15. Test setup of cycloidal gear box

Fig.15 shows circuit to control NEMA 17 stepper motor with Arduino. Stepper motor is powered using a 12V power source, and the A4988 module is powered via Arduino.

4.3 Results

A 3D printed prototype is developed to validate motion analysis. It was actuated by NEMA 17 step motor (0.45 N-m) which is controlled by A4988 motor driver module on the Arduino platform. Tests are conducted on two prototypes as printing of hypocycloidal and epicycloid tooth profile is critical. In first prototype it was observed slipping during rotation and skipping some gear teeth in between and not rotating continuously. Also, the cycloidal disc was rotating out of plane. Gearbox was functioning properly when the motor and cycloidal disc were held at a certain position. One of the main reasons for the above-mentioned problems was the error in assembly that is backlash in meshing cycloidal teeth, this caused problems while rotation. Second prototype components precisely 3D printed and assembled accurately. Problems occurred in first prototype due to backlash are totally rectified. Many test trails are conducted on prototype of cycloidal gear box. Input and output speed were measured through rpm sensor. Displacement trials shows annular gear rotates by 18° during a complete rotation of the input shaft of 360° . The output speed found to be 3 complete rotations in 60 seconds when the input speed of motor was 60 rpm. Motor torque 0.45Nm and output torque found to be 8.82Nm. Kinematic simulation results are very close to the experimental values of speed ratio and torque. Speed, torque and back drivability validated by running gear box at different speed and more than 50 trials. Overall, after 20 rotations of the input shaft, the output shaft completes one rotation. The transmission ratio of the gearbox is thus 20:1 in a very small space of 60 x 60 x 20mm.

5. Conclusion

Design of compact cycloidal gear box is proposed for the application such as humanoid shoulder joints. Research was focused on development of concepts and validation through design, modelling, motion analysis, 3D printing, prototyping and testing. Two out of phase cycloidal gears in assembly helps to reduce vibration and load distribution on individual gears. The output speed found to be 3 complete rotations in 60 seconds when the input speed of motor was 60 rpm. Motor torque 0.45Nm and output torque found to be 8.82 Nm. Also, motion analysis results are very close to the experimental values of speed ratio and torque. Speed, torque and back drivability validated by running gear box at different speed and more than 50 trials. Overall, after 20 rotations of the input shaft, the output shaft completes one rotation. The transmission ratio of the gearbox is thus 20:1 in a very small space of 60 x 60 x 20mm. Proposed cycloid drive exhibits high load capability which is more appropriate for robotic arm applications. Cycloidal gearbox satisfies requirement of humanoid shoulder joints such as high torque, light weight and compact assembly. Additional features noticed are back drivable, vibration and noise free transmission which are highly desirable for humanoid shoulder joints.

References

- [1] Pablo López García, Stein Crispel, Elias Saerens, Tom Verstraten and Dirk Lefeber, "Compact gearboxes for modern robotics: A Review", *Frontiers in Robot and AI*, vol.7, Article 103, August 2020
- [2] Jonathon W. Sensinger and James H. Lipsey, "Cycloid vs. harmonic drives for use in high ratio, single stage robotic transmissions," *IEEE International Conference on Robotics and Automation*, June 2012
- [3] Biser Borislavov, Ivaylo Borisov, Vilislav Panchev, Design of a planetary-cyclo drive speed reducer cycloid stage; geometry; element analyses, Project work report, Linnaeus University, Sweden, May 2012
- [4] Mirko Blagojevic, Nenad Marjanovic, zorica Djordjevic, Blaza Stojanovic and Aleksandar Disic, "A New Design of a Two-Stage Cycloidal Speed Reducer," *Journal of mechanical design*, ASME, vol. 133, no. 8, pp. 085001-12011, August 2011

- [5] Logan C. Farrell, James Holley, William Bluethmann, Marcia K. O'Malley, "Cycloidal gear train in-use efficiency study," ASME, International Design Engineering Technical Conferences and Computers and Information in Engineering Conference, Quebec City, Canada, August 2018.
- [6] Ta-Shi Lai, "Design and machining of the epicycloid planet gear of cycloid drives," The International Journal of Advanced Manufacturing Technology, vol. 28, no.7, pp.665-670, April 2006
- [7] Wei Bo1, Wang Jiayu1, Zhou Guangwu1, Yang Rongsong, Zhou Hongjun and He Tao, "Mixed lubrication analysis of modified cycloidal gear used in the RV reducer," Proc IMechE Part J: Journal of Engineering Tribology, Vol.230 no.2, pp. 121-134, February 2016
- [8] Li Yawei and Wu Yuanzhe, "Design of a cycloid reducer Planetary stage design, shaft design, bearing selection design, and design of shaft related parts," Engineering, Corpus ID 203697900, 2012
- [9] Abhi J. Rawal, Cycloidal-Drive Joint Design for Wearable Exoskeletons, Master Thesis, New Jersey Institute of Technology, December 2020.
- [10] Hiroshi Matsuki, Kenta Nagano and Yasutaka Fujimoto, "Bilateral Drive Gear—A Highly Backdrivable Reduction Gearbox for Robotic Actuators," IEEE/ASME Transactions on Mechatronics, vol. 24, no. 6, pp. 2661-2673, December 2019.
- [11] Benedetto Allotta, Lorenzo Fiorineschi, Susanna Papini, Luca Pugi, Federico Rotini and Andrea Rindi, "Redesigning the cycloidal drive for innovative applications in machines for smart construction yards," World Journal of Engineering vol.18 no.2 pp.302–315, March 2021
- [12] Li, X., Chen, B., Wang, Y., Sun, G. et al., "Geometry Design of a Non-Pin Cycloid Drive for In-Wheel Motor," SAE Technical Paper 2015-01-2172, June 2015
- [13] Wan-Sung Lin, Yi-Pei Shih and Jyh-Jone Lee, "Design of a two-stage cycloidal gear reducer with tooth modifications," Mechanism and Machine Theory, vol.79, 184–197, September 2014
- [14] Nenad Petrovic, Mirko Blagojevic, Nenad Marjanovic, Milos Matejic, "Parametric drawing of a Cyclo drive shortened equidistant Epitrochoid gear," 7th International Quality Conference, Center for Quality, Faculty of Engineering, University of Kragujevac, May 2013.
- [15] Mirko Blagojevic, Nenad Marjanovic, Zorica Djordjevic, Blaza Stojanovic, Vesna Marjanovic, Rodoljub Vujanac, Aleksandar Disic, "Numerical and Experimental analysis of the cycloid disc stress state, UDC/UDK 621.833.058:[519.6:004.421], May 2014.
- [16] Ivan Pantić, Mirko Blagojević, "Kinematic analysis of single-stage Cycloidal speed reducer," Machine
- [17] S.V. Thube and T.R. Bobak, "Dynamic Analysis of a Cycloidal gearbox using Finite Element Method," American Gear Manufacturers Association, ISBN: 978-1-61481-049-0, October, 2012.
- [18] Wear assessment of 3-D printed parts of PLA (Polylactic acid) using Taguchi design and Artificial Neural Network (ANN) technique, Materials Research Express, 25 November 2020